PHYSICAL REVIEW C VOLUME 21, NUMBER 6 JUNE 1980

Neutron total cross section of sulfur: Single level to multilevel to optical model

C. H. Johnson and R. R. Winters*
Oak Ridge National Laboratory, Oak Ridge, Tennessee 37830
(Received 6 February 1980)

This paper is a further analysis of the high resolution total cross section of sulfur for 25–1100 keV neutrons that previously were measured by Halperin, Johnson, Winters, and Macklin and evaluated by single-level analysis. The usual procedure in reporting the results of high resolution neutron cross sections has been to present the data and resonance parameters with corresponding neutron strength functions resulting from some type of R-matrix analysis. Often the important nonresonant phase shifts are not reported. In this paper, making use of both strength functions and phase shifts, we extend the analysis to include an average nuclear potential (a spherical optical model). An optical model analysis not only facilitates comparison with a broad spectrum of other nucleon-nucleus experiments, but also may provide an incentive for microstructure calculations. Six average empirical functions, two each for $s_{1/2}$, $p_{1/2}$, and $p_{3/2}$ partial waves, are derived from the R-matrix analysis. From these we deduce optical model parameters, the real and imaginary well depths for s- and p-wave neutrons, and the spin-orbit well depth for p waves. The resulting real well is deeper for p waves than for s waves and for averages over partial waves at higher energies. The depth of the imaginary wells are about half those deduced at higher energies. An interesting feature of the analysis is that the multilevel curve including interference effects is produced from single-level parameters including the phase shifts.

[NUCLEAR REACTIONS $^{32}S(n,n)$, E_n=25–1100 keV, multilevel analysis of $\sigma_{n,\mathrm{tot}}(E)$, deduced R', strength functions for $l=0$ and 1, optical model parameters for $l=0$ and 1.]

I. INTRODUCTION

The continued importance of the optical model potential (OMP) as a link between experimental and theoretical neutron physics is demonstrated by the microscopic optical potential calculations appearing in the recent literature, e.g., Bernard and van Giai[1] (^{208}Pb), Brieva and Rook[2] (^{40}Ca), Jeukenne, Lejeune, and Mahaux[3] (^{12}C, ^{16}O, ^{27}Al, ^{40}Ca, ^{58}Ni, ^{120}Sn, and ^{208}Pb), Mau and Bouyssy[4] (^{40}Ca), and O'Dwyer, Kawai, and Brown[5] (^{58}Ni). As noted by O'Dwyer *et al.*,[5] the imaginary part of the OMP describes particle-core excitations which can be strongly dependent on the incident particle energy. In this paper we present a spherical OMP analysis of the low energy neutron total cross section for $^{32}S+n$. Using the cross sections and "single-level" resonance parameters reported by Halperin, Johnson, Winters, and Macklin,[6] we produce an R-matrix multilevel curve which describes the $^{32}S+n$ total cross section in detail from 0.025 to 1.1 MeV. From this multilevel curve we deduce the depths of the real and imaginary OMP wells for scattering of s- and p-wave neutrons.

Two results from this work seem to indicate a need for microstructure calculations. Firstly, our absorptive (imaginary) potentials are approximately half as deep as required[7] for sulfur at higher energies. This may be an indication that few particle-core excitations are available at low energies for $^{32}S+n$. Secondly, for the assumed spherical OMP the real well depths are found to be l dependent, perhaps an indication of nuclear deformation and associated collective state excitations.

Section II includes the essential formulas for the single-level description and for the multilevel conversion. Most of these are from standard references on the R-matrix formalism. Using this conversion and the level parameters[6] for those resonances for which definite J^π assignments were made, we calculate a multilevel curve which gives a very good description of the neutron total cross section of sulfur. The procedure does require that a nonresonant phase shift ϕ'_{Jl} be one of the single-level parameters reported for each resonance. This phase contains information relative not only to the conversion to multilevel parameters for the given resonance but also to the interference of the resonance with others of the same J^π, both those observed and those outside of the energy region of the measurements. It is in connection with the outer levels that we introduce a linear smoothed R function $\bar{R}$, which is not familiar in high resolution work but is a standard concept[8] for an OMP.

Section III is an interpretation of the data in terms of an OMP. An OMP, being an average potential, describes averages rather than individual resonances. Most published data relative to the OMP consist of averages over resonances, but high resolution data are needed if one wishes to

study the effects of specific partial waves. Historically[9,10] the most significant high resolution cross section data have been at low neutron energies where s-wave scattering is dominant. From such total cross sections on a given target one can extract two average quantities; the s-wave strength function is found from the average neutron resonance widths and spacings while the scattering radius, usually designated R', is found from the phase shifts observed between resonances. At low energies the s-wave scattering radius is defined as $R' = a_c(1 - \bar{R})$, where a_c is the chosen R-matrix boundary radius. In turn, two OMP quantities can be deduced,[11] e.g., the depths of the real and imaginary wells for an OMP of given geometry.

In this paper, these familiar concepts for low energy s waves are extended to a broader energy region and to higher partial waves. The extension of the strength function is straightforward and familiar; the broader region improves our knowledge of the strength because more levels are included in the average and the higher energies allow higher partial waves to be investigated. The extension of the analog for the scattering radius is more subtle but has been discussed in the literature, e.g., Lane and Thomas.[8] It involves a second average function which accounts for the phase shift which would be observed if all the levels in the energy region under investigation were removed. That phase shift, which could be called "phase-external," is related in the R-matrix formalism to a function "R-external," which is a sum over all outer levels, both *nearby* and *far away*. In the literature the R-external has usually been designated R-infinity R^{∞}_{Jl}, with the implication that only far away states contribute. That notation is appropriate if the measured interval is small such that the effects of levels immediately above and below tend to cancel, leaving only the distant contributions. An extension of measurements to a broader energy region with more levels allows a better determination of R-infinity, which is R-external near the center of the interval. This follows since in the construction of R-external, the truly nearby levels *within* the region are subtracted exactly and the remaining levels just outside the region are less important for the cancellation. However, as the energy is moved away from the center of the interval, the R-external is changed by the imbalance of the contributions of nearby outer levels. Thus, R-external must increase continuously within the interval. This energy dependence contains important information[12]; in fact, it leads to our conclusion that the s-wave absorptive potential is relatively small for ^{32}S.

II. ANALYSIS OF TOTAL CROSS SECTIONS

A. R-matrix formalism

Only elastic neutron scattering is included in the following R-matrix analysis of the neutron total cross section of sulfur (95% ^{32}S) because the energies are below the inelastic threshold and the absorption widths are small relative to the neutron widths of the prominent resonances that enter into the analysis. Also, ^{32}S has zero spin. Thus, the R-matrix for ^{32}S reduces to a single-channel function R_{Jl} for each partial wave. The corresponding total cross section is given by[8]

$$\sigma_{Jl} = 4\pi k^{-2}(J+\tfrac{1}{2})\sin^2\phi_{Jl}, \tag{1}$$

where

$$\phi_{Jl} = \phi_l + \tan^{-1}(P_l R_{Jl}). \tag{2}$$

Here ϕ_l and P_l are the usual hard sphere phase shift and penetrability for l-wave neutrons at the chosen boundary radius. [For simplicity in Eq. (1) we have set the boundary condition B_l equal to the shift factor S_l at all energies.]

The R function is a sum over all levels of the given J^{π}:

$$R_{Jl}(E) = \sum_{\lambda=1}^{\infty} \gamma_{\lambda Jl}^2/(E_{\lambda Jl} - E), \tag{3}$$

where $\gamma_{\lambda Jl}^2$ and $E_{\lambda Jl}$ are the reduced width and eigenenergy, respectively, for the λ^{th} level. We replace this infinite sum by a finite sum over the levels observed in the interval "I" of our measurements plus an R-external for the outer region:

$$R_{Jl}(E) = R^{e}_{Jl}(E) + \sum_{I} \gamma_{\lambda Jl}^2/(E_{\lambda Jl} - E). \tag{4}$$

The above expressions, corrected for experimental resolution and Doppler broadening, could be used with the aid of a sophisticated search routine to produce a detailed multilevel fit to our measurements from 0.025 to 1.1 MeV. An alternate procedure is first to fit each resonance separately and then to convert to the multilevel description. For this purpose Eq. (2) can be rewritten[8] near a level λJl as

$$\phi_{Jl} = \phi'_{Jl} + \tan^{-1}\frac{\Gamma_n/2}{E_0 - E}, \tag{5}$$

where the "non-resonant" phase shift is given by

$$\phi'_{Jl} = \phi_l + \tan^{-1}(P_l R^0_{Jl}), \tag{6}$$

and where

$$\Gamma_n = 2P_l\gamma_{\lambda Jl}^2/d_{Jl}, \tag{7}$$

$$E_0 = E_{\lambda Jl} + P_l R^0_{Jl}\Gamma_n/2, \tag{8}$$

$$R^0_{Jl}(E) = R_{Jl}(E) - \gamma_{\lambda Jl}^2/(E_{\lambda Jl} - E), \tag{9}$$

and

$$d_{Jl} = 1 + (P_l R^0_{Jl})^2 . \quad (10)$$

The R^0_{Jl} is the R function for all but the λJl level. These equations are exactly equivalent to the original multilevel phase in Eq. (2).

B. Single-level analysis

The fitting by Halperin *et al.*[6] of each resonance involved Eqs. (1) and (5) without detailed reference to other resonances as contained in Eqs. (6)–(10). Each level was fit by least-squares adjustment of five parameters: Γ_n, E_0, ϕ'_{Jl}, plus two parameters for a linear background. In a few cases two overlapping levels of different J^π were fit simultaneously. The J and l assignments were discussed.

Some approximations of R^0_{Jl} for other levels are implicit in the fitting procedure. Firstly, the energy dependences of Γ_n and E_0 through R^0_{Jl} are neglected. Secondly, substitution of Eq. (5) into Eq. (1) yields three terms involving the energy dependence of R^0_{Jl}: a Breit-Wigner term, an interference term, and a background term. For the first two terms the R^0_{Jl} is in effect held constant, equal to the value at E_0. But the latter term, which is proportional to $\sin^2\phi'_{Jl}$ and is the partial cross section that would occur if the given resonance were missing, is included in the linear background. Hence an important energy dependence for R^0_{Jl} is effectively included.

C. Multilevel description

The conversion from single to multilevel parameters requires a choice of boundary radius which is essentially arbitrary but, according to the R-matrix formalism, must be outside the polarizing forces. We choose $a_c = 6.4$ fm or $2.016\,A^{1/3}$, a radius at which the real potential for the OMP assumed in Sec. III is 2% of its central value. Table I lists the multilevel parameters $E_{\lambda Jl}$ and $\gamma_{\lambda Jl}{}^2$ calculated for this boundary radius using Eqs. (6)–(10) and the reported[6] parameters for levels of known Jl. Clearly, $E_\lambda = E_0$ and $\gamma_\lambda{}^2 = \Gamma_n/2P_l$ whenever $P_l R^0_{Jl} \ll 1$.

To complete the calculations of the multilevel R function in Eq. (4) we require R-external, $R^e_{Jl}(E)$. At each resonance, we first calculate R^0_{Jl} from the phase shift ϕ'_{Jl} in Eq. (6). That R function includes all but the level at E_0. We then use the level parameters to subtract the contributions of the remaining levels of the same Jl in the interval. The remainders are plotted in Fig. 1. Although the points show fluctuations due to experimental uncertainties, the actual $R^e_{Jl}(E)$ must increase continuously with energy. This behavior is in contrast to the deviations of ϕ'_{Jl} from a smooth curve, which result from nuclear level fluctuations. (Plots of ϕ'_{Jl} were useful for parity assignments.[6]) One could visually draw a smooth curve for $R^e_{Jl}(E)$ to fit the points in Fig. 1 and then adjust this curve to achieve a final multilevel fit to the data. However, our procedure is to introduce a form factor for least-squares fitting of the points and to show that the resulting multilevel curve gives a good description of the cross sections. The chosen form factor serves also to introduce the OMP.

TABLE I. Multilevel R-matrix parameters and compound excitation energies for $^{32}S + n$ resonances of definite J^π for boundary radius $a_c = 6.4$ fm.

J^π	E_λ (keV lab)	$\gamma_\lambda{}^2$ (keV lab)	E_{exc} (keV)
$\frac{1}{2}^-$	30.38	2.50	8671.7
$\frac{3}{2}^-$	97.50	0.90	8736.7
$\frac{1}{2}^+$	101.37	17.72	8740.5
$\frac{3}{2}^-$	112.18	3.54	8751.0
$\frac{1}{2}^-$	202.63	9.09	8838.6
$\frac{1}{2}^-$	272.09	3.48	8906.0
$\frac{3}{2}^-$	288.36	2.20	8921.7
$\frac{1}{2}^+$	375.32	5.16	9006.0
$\frac{3}{2}^-$	412.33	0.10	9041.9
$\frac{5}{2}^+$	462.76	0.73	9090.8
$\frac{5}{2}^+$	586.87	6.80	9211.1
$\frac{5}{2}^+$	649.24	2.09	9271.6
$\frac{5}{2}^+$	675.37	1.07	9296.9
$\frac{1}{2}^+$	693.21	6.38	9314.2
$\frac{1}{2}^-$	724.74	3.38	9344.8
$\frac{3}{2}^-$	740.78	0.84	9360.3
$\frac{3}{2}^-$	778.58	1.02	9397.0
$\frac{5}{2}^+$	818.71	1.57	9435.9
$\frac{5}{2}^+$	919.85	1.80	9533.9
$\frac{3}{2}^-$	920.66	1.72	9534.7
$\frac{5}{2}^+$	947.23	2.19	9560.5
$\frac{1}{2}^-$	984.58	4.74	9596.7
$\frac{1}{2}^-$	1007.84	0.87	9619.2
$\frac{1}{2}^+$	1045.97	1.10	9656.2
$\frac{1}{2}^-$	1048.50	1.36	9658.7
$\frac{5}{2}^+$	1055.28	2.27	9665.2
$\frac{1}{2}^+$	1064.78	0.13	9674.4
$\frac{3}{2}^-$	1091.39	0.23	9700.2

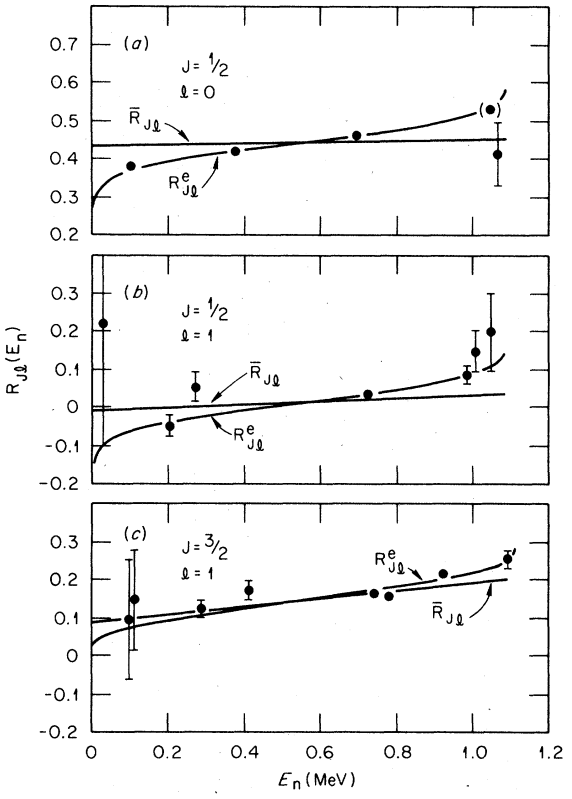

FIG. 1. Experimental and empirical external R functions and corresponding smoothed $\bar{R}$. The points show the experimental R^e_{JI}; the point in parenthesis represents one member of a close doublet (see Ref. 6) that was not included for fitting R_{JI}. The curves are the empirical best fits to R^e_{JI} and corresponding linear $\bar{R}_{JI}$ deduced with the internal strengths equal to the observed values from Fig. 1. Parameters are listed in Table II.

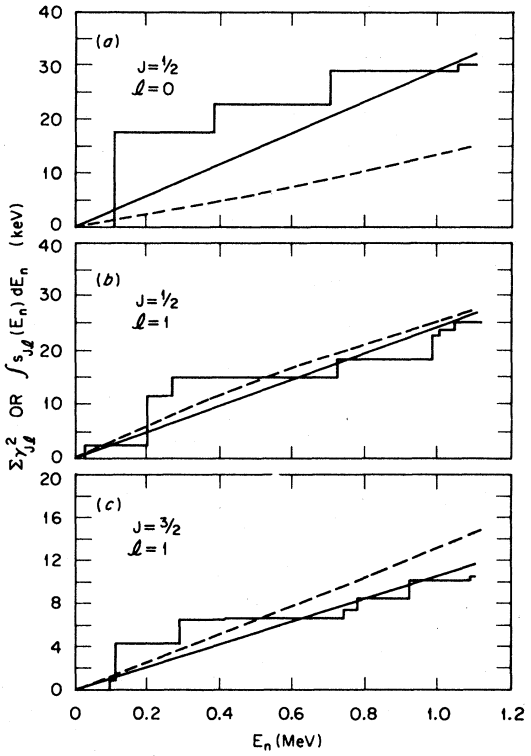

FIG. 2. Integrated reduced widths for s- and p-wave resonances. The step plots show the summations of observed reduced widths and the solid straight lines are best-fit ourves. The strength functions of slopes of these curves are listed in Table II. The dashed curves are for the best-fit optical model potentials; the corresponding fits to R-external are shown in Fig. 5.

An analytic form factor is needed. If the actual discrete levels are replaced by a continuous density of reduced width, i.e., the strength function $s_{JI}(E)$, then a smoothed real R function can be defined:

$$\bar{R}_{JI}(E)=\mathrm{Pr}\int_{-\infty}^{+\infty} s_{JI}(E')dE'/(E'-E), \qquad (11)$$

where Pr signifies the "principle part." The external R function is then

$$R^e_{JI}(E)=\bar{R}_{JI}(E)-\mathrm{Pr}\int_{I} s_{JI}(E')dE'/(E'-E), \qquad (12)$$

where the integral is over the measured interval I.

In Sec. III we use an OMP to generate $\bar{R}_{JI}(E)$ and $s_{JI}(E)$ but in this section we use a more empirical approach. To evaluate the integral in Eq. (12) we need the average experimental strength function, $\langle\gamma^2/D\rangle\approx s_{JI}(E)$. Figure 2 shows conventional step plots of the summed reduced widths versus energy for partial waves, $s_{1/2}$, $p_{1/2}$, and $p_{3/2}$. Also shown are linear least-squares fits obtained using weighting factors discussed by Halperin[6] and in Sec. III. The strength functions, which are the slopes of the curves, are listed in Table II and are used to evaluate the above integral. We then fit $R^e_{JI}(E)$ from Eq. (12) by least squares to the data of Fig. 1, under the assumption that $\bar{R}_{JI}(E)$ is linear with two adjustable parameters, i.e.,

$$\bar{R}_{JI}(E)=\alpha_{JI}+\beta_{JI}E. \qquad (13)$$

TABLE II. Parameters for the empirical external R function.[a]

JI	s_{JI}	α_{JI}	β_{JI} (MeV^{-1})
$s_{1/2}$	0.029	0.43	0.018
$p_{1/2}$	0.025	−0.010	0.041
$p_{3/2}$	0.011	0.088	0.11

[a]Equations (12) and (13) with integral limits 0 to 1.1 MeV.

Figure 1 shows the fitted R^e_{Jl} curves with corresponding $\bar{R}_{Jl}$, and Table II lists the best-fit parameters.

Figures 3 and 4 show the resulting multilevel curves for natural sulfur (0.95% ^{32}S) calculated from the equation

$$\sigma_{n,\mathrm{tot}} = \sum_{Jl} (0.95\sigma_{Jl} + 0.05\bar{\sigma}_{Jl}), \tag{14}$$

where σ_{Jl} is calculated for ^{32}S from Eqs. (1), (2), (4), (12), and (13) with parameters from Tables I and II, and $\bar{\sigma}_{Jl}$ is an average approximation for the minor isotopes for which R_{Jl} is replaced by $\bar{R}_{Jl}$. Eight d-wave resonances[6] are included; the nonresonant d-wave cross sections are negligible. Excluded from this curve are the minor resonances of uncertain J^π, the effects of Doppler and resolution broadening, and all resonances for minor isotopes. The small broad peaks near energies of 0.3, 0.36, 0.4, 0.8, and 0.85 MeV are attributed to ^{34}S. The multilevel curve gives a good description of the data, including the broad interfering resonances.

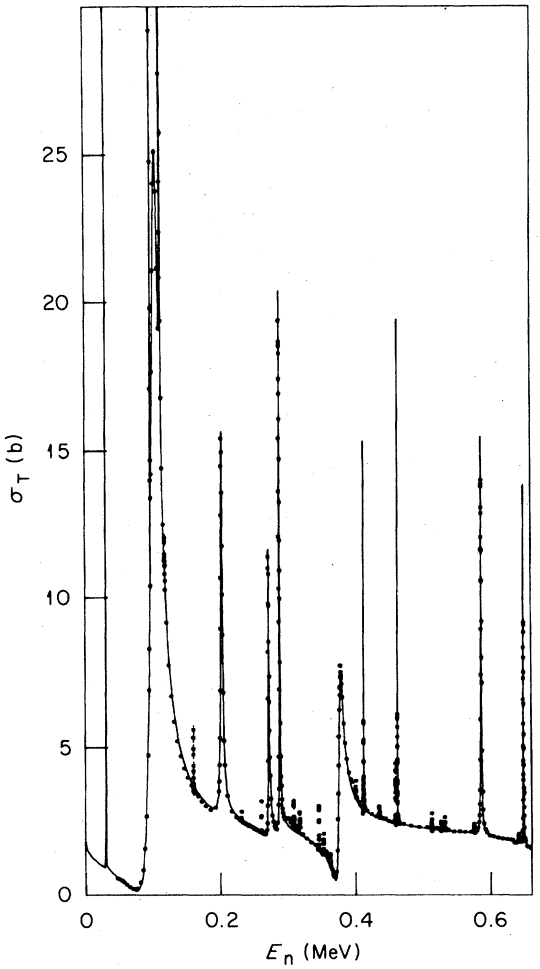

FIG. 3. Experimental cross sections and multilevel curve for neutrons on sulfur. The data from Ref. 6 have been averaged over many energy channels wherever no resonances were observed. The multilevel curve was deduced from the single-level analyses of Ref. 6. It does not include the effects of Doppler or resolution broadening, the minor resonances in ^{32}S, and all resonances in the minor isotopes.

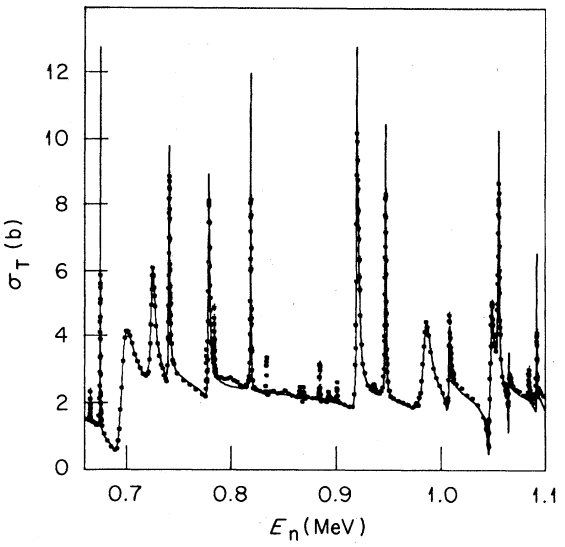

FIG. 4. Continuation of Fig. 3.

If for some reason a different boundary radius were desired, it would be necessary to regenerate Tables I and II from the single-level parameters.[6] Essentially the same multilevel curve should result.

We emphasize that, even though the use of the single-level formalism with the subsequent multilevel conversion gives considerable insight and is often convenient (as it was in the present study), a direct multilevel least-squares fit to the data would certainly be feasible and would give the same parameters. Suitable search parameters for the R-external of Eqs. (12)–(13) would be the α_{Jl} and β_{Jl} for the smoothed R function. The strength s_{Jl} for the integral would be fixed at a reasonable value deduced either from a preliminary analysis of the resonances or from the literature. Generally the exact value for s_{Jl} is not critical because it is highly correlated with β_{Jl}.

III. OPTICAL MODEL ANALYSIS

If an average neutron-nucleus potential is assumed, the neutron scattering matrix elements $\bar{U}_{Jl}$ can be calculated. If only elastic neutron scattering is allowed, the matrix elements can be expanded in terms of average complex R func-

tions[8]:

$$\bar{U}_{Jl}=e^{2i\phi_l}\frac{1-L_l^*\bar{R}_{Jl}}{1-L_l\bar{R}_{Jl}}, \tag{15}$$

where $L_l=S_l-B_l+iP_l$, S_l is the shift factor evaluated at the boundary radius, and B_l is the boundary condition. The boundary conditions must be the same as used for the R-matrix analysis, namely $B_l=S_l$ at all energies and $a_c=6.4$ fm. Also the assumed OMP must be negligible for $r>a_c$.

The complex R functions can be written

$$R_{Jl}=\bar{R}_{Jl}+i\pi s_{Jl}, \tag{16}$$

where, as shown by Lane and Thomas,[8] the s_{Jl} corresponds to the strength function of the actual fine structure averaged over many levels and $\bar{R}_{Jl}$ is the smoothed R function defined by Eq. (11).

For the average potential we use for each J^π a spherical optical model consisting of real Woods-Saxon and spin-orbit terms plus an imaginary surface term. In order to satisfy the requirement of the R-matrix formalism, i.e., that our channel radius a_c be truly outside the range of the nuclear forces, we cut off the potential at a radius $r_c=2.01A^{1/3}$ which is slightly smaller than a_c. Thus, our potential has the form, for $r<r_c$,

$$V^l(r)=V_0^l f(r)+V_{so}\frac{\vec{\sigma}\cdot\vec{l}}{r}\left(\frac{\hbar}{m_\pi c}\right)^2\frac{d}{dr}f(r)$$

$$+i4a_D W_D^{Jl}\frac{d}{dr}g(r)$$

and

$$V^l(r)=0 \quad \text{for } r\geq r_c,$$

where

$$f(r)=\{1+\exp[(r-R_0)/a_0]\}^{-1},$$
$$g(r)=\{1+\exp[(r-R_D)/a_D]\}^{-1}, \tag{17}$$
$$R_0=r_0A^{1/3} \text{ and } R_D=r_DA^{1/3}.$$

Since the model with its seven parameters for each l value is overparametrized for the present study, we must fix some values at the outset. Our choice is to fix all four geometric parameters at the values deduced by Holmqvist[7] from a systematic study of neutron elastic scattering in the energy region of 1.5 to 8.1 MeV. These values are similar to others in the literature[13] and are listed in Table III. Our OMP calculations were done using the computer code SCAT.[14]

With this model we fit the observed R external and strength functions by least-squares adjustments of V_0^l and W_D^l for $s_{1/2}$ waves and of V_0^l, V_{so}, and W_D^{Jl} for $p_{1/2}$ and $p_{3/2}$. The criterion for the OMP best fits for each l value was the minimization of the chi-squared statistic

$$\chi_\nu^2=\chi_\nu^2(R_{Jl}^e)+\chi_\nu^2(s_{Jl}), \tag{18}$$

where $\chi_\nu^2(R_{Jl}^e)$ and $\chi_\nu^2(s_{Jl})$ are the usual reduced chi-squared estimators for fits to the R external and strength function, respectively. The weights for the fits to R external were the reciprocal of the variances deriving from the variances for the single-level phase shifts. However, the relatively small experimental variances associated with the reduced widths underestimate the uncertainty in the estimate of s_{Jl}. Liou and Rainwater[15] discuss this problem and provide estimates of the uncertainty for s_{Jl}. The OMP and empirical least-squares (Sec. II) fits to the integrated strengths were weighted with the variance estimators of Liou and Rainwater. For the OMP fitting, this weighting largely removed the bias toward minimizing $\chi_\nu^2(s_{Jl}^l)$ which would result if the experimental variances of the reduced widths had been used. The best-fit values are listed in Table III. The corresponding curves for the strengths are shown by the dashed lines in Fig. 2. Figure 5 shows the $R_{Jl}^e(E)$ and corresponding $\bar{R}_{Jl}(E)$. The multilevel curves resulting from the OMP analysis are almost indistinguishable from those plotted in Figs. 3 and 4. The $R_{Jl}^e(E)$ in Fig. 5 are essentially the

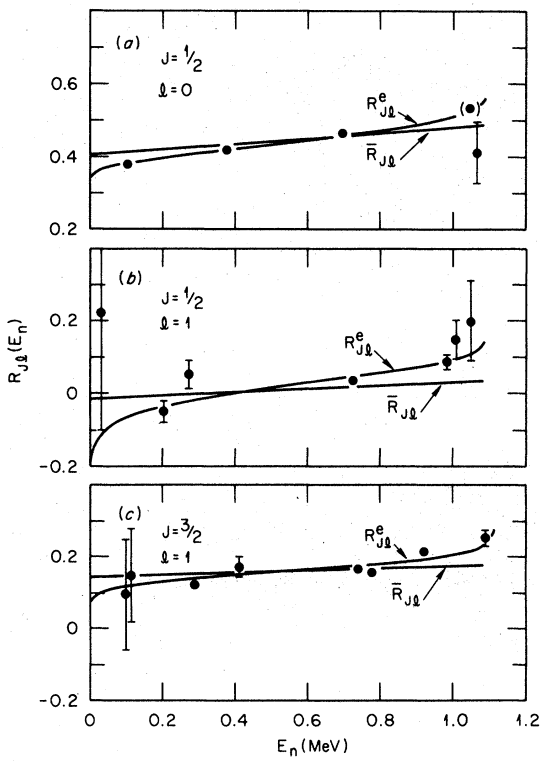

FIG. 5. Optical model fits to the external R functions. The figure is similar to Fig. 1 except that the curves are deduced from the optical model potential.

TABLE III. Fixed and best-fit optical model parameters.

Fixed geometries (fm)	Best-fit depths (MeV) s waves	p waves
$r_0 = 1.21$	$V_0 = 53.8 \pm 0.4$	$V_0 = 62.4 \pm 1.1$
$a_0 = 0.66$	$W_D = 3.0 \pm 1.3$	$V_{s0} = 13 \pm 3$
$r_D = 1.21$		$W_D(p_{1/2}) = 2.6 \pm 1.1$
$a_D = 0.48$		$W_D(p_{3/2}) = 4.5 \pm 1.8$

same as in Fig. 1 but the $\overline{R}_{Jl}(E)$ are different, particularly for s waves, as discussed below.

IV. DISCUSSION OF THE OPTICAL MODEL

A. A possible nonstatistical component for the 101-keV resonance

The resonance at 101 keV contains more than half of the total reduced width for the five s-wave resonances and its width is about 1% of the 3s single particle width. Moreover, Halperin *et al.*[6] report that it has a non-negligible valency capture component. If that one level were a nonstatistical state, the observed average strength with this level included would not properly represent the strength function. Further information on the correct strength function is contained in the R external because it depends partly on the strength just outside the measured region. Furthermore, the R external has a relatively small uncertainty, particularly for s waves for which a small change in $R^e(E)$ would produce an obvious misfit to the cross sections. For the empirical s-wave fit in Sec. II the nearly constant $\overline{R}$ requires that the external strengths above and below the measured interval be the same as the observed internal average. In contrast, the OMP analysis in Sec. III requires, as indicated by the dashed curve in Fig. 2, that the outer strengths be about half of the internal average. Since the observed strength could be reduced to the OMP value if the 101-keV resonance were omitted, this OMP analysis indicates that the resonance is nonstatistical.

This prediction from the OMP is clarified by Fig. 6, which shows $s(E)$ and $\overline{R}(E)$ for s waves calculated up to 8 MeV using constant well depths from Table III. The energy of the 3s resonance is a function of the assumed boundary radius, 6.4 fm, and of the parameters of the real well; the spreading width is a function of the imaginary potential. Also shown is the fitted $R^e(E)$ from Fig. 5(a). It deviates from $\overline{R}(E)$ towards both ends of the interval, but the deviations are small because $s(E)$ is small, i.e., only about half of the observed average. The OMP $s(E)$ can be increased to equal the observed average, *without* disturbing the average $\overline{R}$,

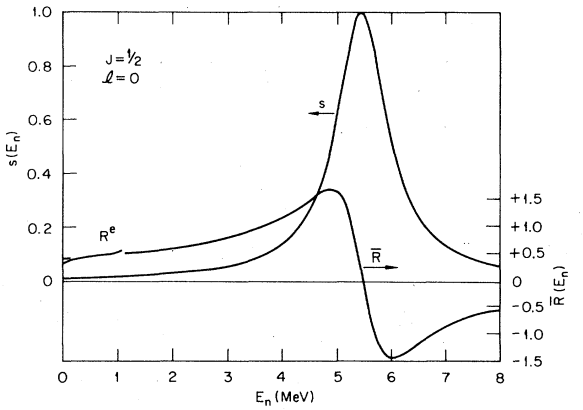

FIG. 6. Predictions of $\overline{R}(E_n)$ and $s(E_n)$ for the best fit s-wave potential. The well depths are held constant with $V_0 = 53.8$ MeV and $W_D = 3.0$ MeV. The resonance energy of 5.45 MeV for the 3s state depends on the 6.4 fm boundary radius as well as the volume of the real well. The interval of the measurement is only 0 to 1.1 MeV and the external function R^e shown for the interval is the same as in Fig. 5.

by increasing W_D about a factor of 2 and making a slight adjustment in V_0. But the $R^e(E)$ then deviates more strongly from $\overline{R}(E)$ and the multilevel curve is a poor description of the cross sections.

B. Real well l dependence

The real well depths are determined primarily from the phase-external or corresponding R external. A particularly interesting result of this study is that the real well for p waves is deeper than for s waves by about 16%. The s-wave depth of 53.8 MeV is about as expected from other OMP studies. For example, if our s-wave potential depth is used with the isospin term[16] $24(N-Z)/A$ MeV subtracted, it predicts the peak of the 3s size resonance at $A = 52$, in good agreement with the observed[10] maximum near $A = 55$. At higher energies (6, 7, and 8 MeV) Holmqvist[7] scattered neutrons from sulfur and, using the present OMP geometry, deduced a 50-MeV depth. (This represents an average for all partial waves.) The difference from our 53.8-MeV for s waves could be attributed to a linear term in an energy dependent real well depth with coefficient 0.58 MeV^{-1}, a reasonable value[17,18] for ^{32}S.

These comparisons suggest that our p-wave well depth is unusually deep. But if the p-wave depth were reduced to the s-wave value, the $2p_{1/2}$ single particle state would become unbound by about 500 keV and the strength would be much larger than observed. In other words, the 2p size resonance would be near $A = 32$. The deeper well binds the p-states and, although this may not agree

with other OMP studies, it is consistent with (d,p) stripping measurements, which have shown that most of the $2p$ strength is in the bound region. Mermaz *et al*[19] measured $^{32}S(d,p)$ stripping for 18-MeV deuterons and deduced spectroscopic factors, some tentative, for four $p_{1/2}$ levels and six $p_{3/2}$ levels. The summed spectroscopic factors were nearly unity, 1.01 for $p_{1/2}$ and 0.91 for $p_{3/2}$, and the energy centroids weighted by the spectroscopic factors were −2.4 MeV for $p_{1/2}$ and −4.0 MeV for $p_{3/2}$. (These quantities may have large uncertainties.) It is of interest to compare these centroids with the eigenenergies for our p-wave OMP. The real part of our OMP binds the $2p_{1/2}$ state at −2.0 MeV and the $2p_{3/2}$ at −5.7 MeV.

If the s-wave well were increased to the p-wave depth of 62.4 MeV, the $3s$ resonance in Fig. 6 would move down to 2.5 MeV. Both $\overline{R}(E)$ and $s(E)$ would then be too large relative to the experiment.

It is reasonable to believe that another model, say a nonspherical OMP, could remove the l dependence in the real well. Given the 6.4 fm R-matrix boundary, the model would be required to reproduce the average strengths and external R functions reported here.

C. Small absorptive potentials

The imaginary well depths of about 3 MeV for both s and p waves are a factor of 2 or 3 smaller than usually found in OMP studies. For example, Holmqvist[7] found $W_D = 6$ to 10 MeV for neutron scattering from sulfur at 6, 7, and 8 MeV. But a small well depth may be reasonable at low energies if particle-core states are not easily reached. In the theory[1-5] of the OMP the absorptive or imaginary potential arises from processes in which the incident particle excites the core to states in which the energy of the excited core-plus-particle is approximately equal to the incident energy of the particle. A likely candidate for $\frac{1}{2}^+$ particle-core states near the energy region studied here would be a $d_{3/2}$ particle coupled to the 1^+ excited ^{32}S core consisting of a $d_{3/2}$ particle and $d_{5/2}$ hole. The 1^+ or $M1$ strengths in the ^{32}S core have been observed[20] at 8.13, 10.82, 11.14, and 11.62 MeV with $M1$ strengths 2.8, 2.9, 18.9, and 9.7 eV, respectively. Since very little of the reported $M1$ strength is contained in the range of excitation energies 8.6–9.7 MeV of our work, a small W_D might be expected if states which de-excite by $M1$ transitions dominate. More detailed microstructure calculations of these and other particle-core excitations should be made. Even without such detailed calculations, we expect that the s-wave imaginary well depth would increase significantly over the next 2 MeV of excitation as the bulk of the $M1$ strength is encountered.

D. R-matrix boundary radius invariance

It is emphasized that the optical model parameters are expected to be independent of the assumed R-matrix boundary radius, providing the radius is outside the potential. We investigated this by repeating the analysis using the same model form factors but with the boundary radius a_c increased to 7.4 fm. The best fit OMP well depths were unchanged.

E. Scattering radius

A real potential phase shift can be defined

$$\phi_{Jl}^{\text{pot}} = \phi_l + \tan^{-1}(P_l \overline{R}_{Jl}). \tag{19}$$

In general this differs from the real part ϕ_{Jl}^{real} of the complex phase shift for the OMP. However, at low energies where $P_l s_{Jl}$ is negligible and with the boundary conditions $B_l = S_l$, these two real phases become equal. It follows from the foregoing discussion that the low energy potential phase is independent of the assumed boundary radius a_c. The scattering radius is then given by

$$R' = k^{-1}\phi_{l=0}^{\text{real}} \simeq a_c(1 - \overline{R}_{l=0}). \tag{20}$$

For the s-wave OMP we find in the limit $E \to 0$, $R' = 3.80$ fm. A compilation of low energy data[10] gives $R' = (4.1 \pm 0.2)$ fm, in good agreement with our result.

ACKNOWLEDGMENTS

We are grateful to Dr. D. J. Horen and Dr. R. L. Macklin for many helpful discussions. We are also indebted to Dr. J. A. Harvey and Dr. E. G. Perey for careful and critical reading of this manuscript.

This work was sponsored by the Division of Basic Energy Sciences, U. S. Department of Energy under Contract No. W-7405-eng-26 with the Union Carbide Corporation and Contract No. EY-76-5-02-2696 with Denison University.

*Present address: Denison University, Granville, Ohio 43203.

[1] V. Bernard and Nguyen van Giai, Nucl. Phys. A327, 397 (1979).

[2] F. A. Brieva and J. R. Rook, Nucl. Phys. A291, 317 (1977).

[3] N.-P. Jeukenne, A. Lejeune, and C. Mahaux, Phys. Rev. C 16, 80 (1977).

[4] N. Vinh Mau and A. Bouyssy, Nucl. Phys. A257, 189 (1976).

[5]T. F. O'Dwyer, M. Kawai, and G. E. Brown, Phys. Lett. 41B, 259 (1972).
[6]J. Halperin, C. H. Johnson, R. R. Winters, and R. L. Macklin, Phys. Rev. C 21, 545 (1980).
[7]B. Holmqvist, Ark. Fys. 38, 403 (1968).
[8]A. M. Lane and R. G. Thomas, Rev. Mod. Phys. 30, 257 (1958).
[9]*Experimental Neutron Resonance Spectroscopy*, edited by J. A. Harvey (Academic, New York, 1970).
[10]*Resonance Parameters*, 3rd ed., compiled by S. F. Mughabghab and D. I. Garber, BNL Report No. 325 (National Technical Information Service, Springfield, Virginia, 1973), Vol. 1.
[11]J. E. Lynn, *Theory of Neutron Resonance Reactions* (Clarendon, Oxford, 1968).
[12]F. W. K. Firk, J. E. Lynn, and M. C. Moxon, Proc. Phys. Soc. (London) 82, 477 (1963).
[13]C. M. Perey and F. G. Perey, At. Data and Nucl. Data Tables 17, 1 (1976).
[14]W. R. Smith, Comput. Phys. Commun. 1, 106 (1969).
[15]H. I. Liou and J. Rainwater, Phys. Rev. C 6, 435 (1972).
[16]G. R. Satchler, in *Isospin in Nuclear Physics*, edited by D. H. Wilkinson (North-Holland, Amsterdam, 1969), Chap. 9.
[17]F. G. Perey, Phys. Rev. 131, 745 (1963).
[18]P. H. Stelson and L. Grodzins, Nucl. Data Sect. A 1, 21 (1965).
[19]M. C. Mermaz, C. A. Whitten, Jr., J. W. Champlin, A. J. Howard, and D. A. Bromley, Phys. Rev. C 4, 1778 (1971).
[20]L. W. Fagg, Rev. Mod. Phys. 47, 683 (1975).